TP Experimental TMA 2025-26

Louis Chailleux

January 2026

Contents

1 Lab Report Intro

1.1 English intro

The following lab report presents four experiments either performed by, or demonstrated to, students in the Turbulence: Methods and Applications course (2025–2026). The primary objective of these labs was to provide hands-on experience with turbulence and highlight the diversity of physical contexts in which turbulence plays a critical role.

Throughout these experiments, students acquired, processed, and analyzed experimental data, as well as observed more complex experimental setups through demonstrations. These activities contributed to the development of essential skills required to characterize and understand turbulence, including data acquisition, in-situ experimental measurements, and the use of high-speed imaging techniques.

On the data analysis side, several fundamental tools and methods commonly used in turbulence research were introduced and applied. These included statistical analysis through probability density functions, spectral analysis using power spectral density functions, and signal processing techniques such as Hanning windows and Gaussian kernels. A dedicated section of this report provides further explanation of these technical aspects and their relevance to turbulence analysis.

1.2 French intro

Le rapport de laboratoire suivant présente quatre expériences réalisées par, ou démontrées aux étudiants dans le cours Turbulence : Méthodes et applications (2025–2026). L'objectif principal de ces laboratoires était d'offrir une expérience pratique des écoulements turbulents et de mettre en évidence la diversité des contextes physiques dans lesquels la turbulence joue un rôle central.

Tout au long de ces expériences, les étudiants ont acquis, traité et analysé des données expérimentales, ainsi qu'observé des configurations expérimentales plus complexes par le biais de démonstrations. Ces activités ont contribué au développement des compétences essentielles nécessaires pour caractériser et comprendre la turbulence, y compris l'acquisition de données, les mesures expérimentales in situ et l'utilisation de techniques d'imagerie à grande vitesse.

Du côté de l'analyse des données, plusieurs outils et méthodes fondamentaux couramment utilisés dans la recherche sur la turbulence ont été introduits et appliqués. Il s'agit notamment de l'analyse statistique par le biais des fonctions de densité de probabilité, de l'analyse spectrale à l'aide des fonctions de densité du spectre de puissance et des techniques de traitement du signal telles que les fenêtres d'Hanning et les noyaux gaussiens. Une section dédiée de ce rapport fournit des explications supplémentaires sur ces aspects techniques et leur pertinence pour l'analyse de la turbulence.

2 Background Technical information

2.1 Spectral Analysis

Spectral analysis methods are essential for studying the distribution of turbulent energy across scales. Power spectral density (PSD) functions are computed from time-resolved signals to examine how energy is distributed as a function of frequency. In turbulent flows, these spectra often exhibit characteristic scaling laws, such as the Kolmogorov -5/3 slope in the inertial sub range, quantifying the cascade of energy from large to small scales.

2.2 Statistical description of turbulence

Turbulent flows can be characterized fluctuating velocity and thus cannot be fully described using instantaneous quantities alone. Statistical tools are therefore necessary to characterize their behavior. Probability density functions (PDFs) are used to analyze the distribution of velocity or scalar fluctuations and is used to identify deviations from Gaussian behavior, this may indicate intermittency or anisotropy in the flow. Mean values, variances, and higher-order moments provide quantitative measures of turbulence intensity and variability.

2.3 Signal processing techniques

In order to improve the quality of the spectral estimates, noise reduction techniques are applied prior to analysis. Windowing functions, such as the Hanning window, are used to limit spectral leakage caused by finite signal lengths. Gaussian kernels are employed for smoothing and filtering signals, allowing clearer identification of dominant scales and trends while preserving the underlying physical behavior.

2.4 In-situ measurements

Multiple experiments relied on using in-situ time based instruments, through anemometers,thermocouples and high speed cameras. The anemometers (Pitot tube or sonic variety) provided air velocity at high sample rates. Coupled with the thermocouples, which provided precise temperature data, these two combined offer high temporal resolution and are particularly suited for turbulence statistics and spectral analysis. for long durations. High speed camera provided visualizations of rapidly evolving turbulent flows, which allowed for the analysis of flow structures and velocity fields.

3 TP sillages

Flow behind a cylinder is a canonical problem in the study of turbulent wakes. In this experiment, a 4 cm diameter cylinder was placed at the entrance of the test section of a closed-loop wind tunnel, disrupting an initially homogeneous freestream (2). The resulting velocity fluctuations in the wake were measured using a three-dimensional Cobra anemometer probe, which can be positioned precisely in vertical and horizontal direction. Different Reynolds numbers were studied and achieved by varying the wind tunnel velocity. For each flow condition, velocity time series were recorded at multiple spatial locations from the cylinder, allowing statistical convergence and spectral analysis of the turbulent fluctuations. A 4cm diameter cylinder was placed at the entrance of the .75m x .75m square testing section. The cylinder was placed at mid height and ran along the depth of the testing section. The closed loop wind tunnel covered inwards towards the testing section, then looped back around by going through a tranquility chamber where honeycomb and grid structures homogenized the flow. The cobra anemometer was then digitally controlled in the vertical and horizontal direction as to allow for the gathering of 100s of data per run. For each Reynolds number measurements were taken at different horizontal and vertical points from the cylinder. These were taken in intervals of 10mm. A pitot tube at the end of the testing section was used to gather the bulk flow data of the wind tunnel and was used to determine the wind tunnel velocity. In the resulting spectra 2 a first peak is present at 15hz, this is a result of Von karman shedding. A second peak is found at 22hz, which is a result of Kelvin-helmotz instability.

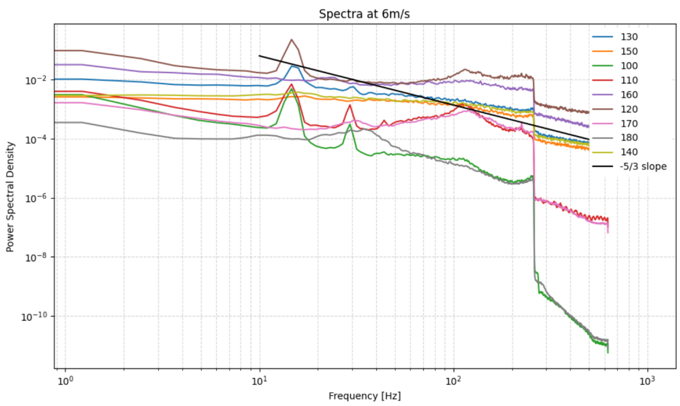

Figure 1: Shows Power spectral density of the velocity fluctuations measured at several spatial positions for a freestream velocity of approximately 6 m/s. The sharp cut off at approximately 280hz is explained due to lowpass filtering being done by the Cobra anemometer.

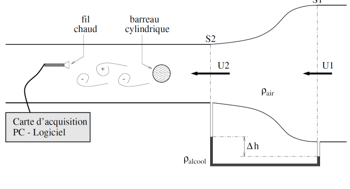

Figure 2: Shows the experimental set up.

4 TP Spray

Jet atomization plays a critical role in many industrial applications; however, characterizing the resulting spray remains challenging due to its highly turbulent nature. The near-field region, defined as the area closest to the nozzle exit, strongly influences the downstream spray structure and breakup behavior. The objective of this experiment was to observe the early development of a liquid jet, identify dominant flow structures, and evaluate spray stability and atomization mechanisms. A two-phase flow was generated using a spray nozzle composed of a central liquid jet surrounded by a co-flowing gas stream (Fig. 4). The large velocity difference between the two phases induces shear instabilities that promote surface deformation and breakup of the liquid core. A high-speed camera was used to capture the temporal evolution of the spray near the nozzle exit. The recorded images were processed using image analysis techniques to estimate the liquid core length and characterize breakup dynamics (3. The observed breakup behavior is consistent with shear-driven instabilities commonly reported in atomizing jets. In particular, the interaction between the fast gas stream and the liquid jet generates Kelvin–Helmholtz-type disturbances that grow in amplitude and ultimately lead to fragmentation of the liquid column.

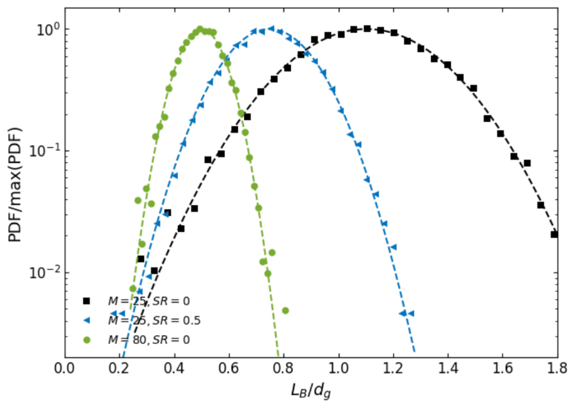

Figure 3: This shows the PDF of the jet core length L_B normalized by the nozzle diameter d_g.Note the higher the M the more spread out the PDF becomes.

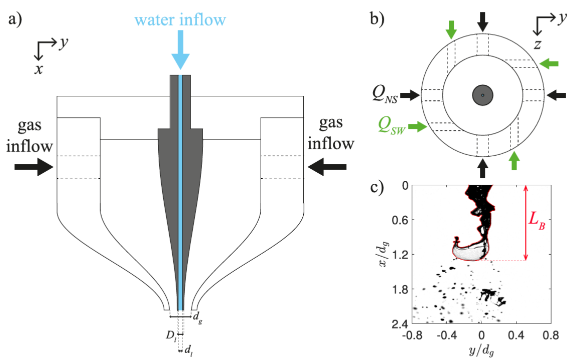

Figure 4: Experimental set up

5 TP Grille Oscillante

An oscillating grid experiment was used to generate a nearly homogeneous and isotropic turbulent flow in water and to study the dynamics of tracer particles using Lagrangian particle tracking. High-speed imaging was used to record particle trajectories for several forcing frequencies. Particle positions were extracted and smoothed using Gaussian filtering prior to numerical differentiation to obtain velocity and acceleration signals. Basic statistics such as mean values, root-mean-square (RMS) fluctuations, and probability density functions (PDFs) were analyzed. The experiment consisted of a see through water container with an oscillating grid placed inside (5). The speed of the grid was controlled by the voltage of power supply. Particles were then diluted into a soap solvent. The mixture was then injected into the container. The particles were then tracked by a high speed camera. A calibration image of a ruler immersed in the tank provided the spatial conversion factor between pixels and physical length. Image sequences were recorded for each forcing condition with appropriate frame rate and exposure time to minimize particle blur and inter-frame displacement. Particle trajectories were reconstructed using a tracking algorithm. To reduce differentiation noise, the raw position signals were smoothed using a Gaussian convolution kernel. Velocities were obtained by differentiating the smoothed positions, and accelerations were computed using a doubly differentiated Gaussian kernel. Probability density functions of the velocity fluctuations were approximately symmetric and close to Gaussian when normalized by their standard deviation. In contrast, acceleration PDFs displayed broader tails, reflecting intermittency and the presence of strong small-scale fluctuations. The acceleration statistics were sensitive to the width of the differentiation kernel, demonstrating the trade-off between noise reduction and temporal resolution.

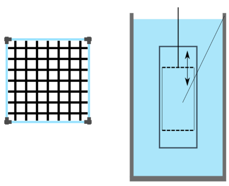

Figure 5: Sketch showing the experimental set up.

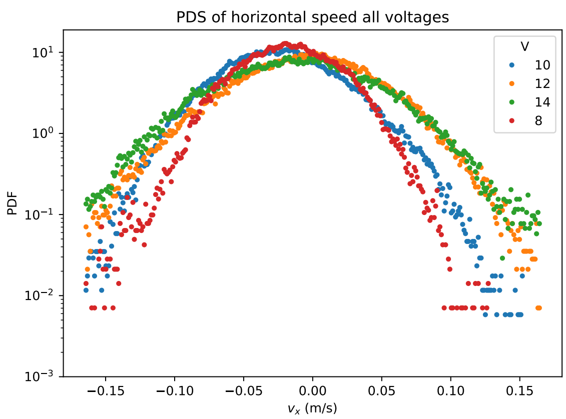

Figure 6: Probability density function of particle speeds compared with each test case

6 TP Couche Limite Atmospheric

6.1 Abstract

La couche limite atmosphérique (CLA) désigne la partie la plus basse de l'atmosphère terrestre, où elle échange de la quantité de mouvement, de la chaleur et de l'humidité avec la surface de la Terre. Ces interactions avec l'océan et la terre font de la CLA un élément clé pour comprendre l'environnement et le climat. Dans cette couche, un fort transport turbulent se produit qui affecte ensuite la distribution de la température et les vents proches de la surface. En raison de sa nature turbulente, caractériser et modéliser la couche limite atmosphérique est particulièrement difficile et pose de nombreux défis. Ce laboratoire explore les propriétés turbulentes de l'CLA expérimentalement in situ dans la chaîne de montagnes des Alpes de Belledonne.

Atmospheric boundary layer (ABL) refers to the lowest portion of the Earth's atmosphere, where it exchanges momentum, heat and moister with the Earth's surface. These interactions with the ocean and land make ABL a key component in understanding the environment and climate. Within this layer, strong turbulent transport occurs which then affects temperature distribution and near-surface winds. Due to its turbulent nature, characterizing and modeling the atmospheric boundary layer is particularly challenging and poses many challenges. This lab explores the turbulent properties of the ABL experimentally in situ in the Belledonne Alps mountain range.

6.2 Background/Introduction

The atmospheric boundary characteristics vary considerably throughout the diurnal cycle. Notably its height will vary between a few hundred meters throughout the night and extend to 2 kilometers throughout the day. This phenomenon is caused by solar heating generating a positive sensible heat flux, leading to buoyancy-driven turbulence and convective vertical currents. This extends the atmospheric boundary layer vertically and encourages vertical mixing, resulting in unstable atmospheric conditions. At night, the absence of solar heating leads to radiation driven cooling of the surface and air near the ground. This process suppresses vertical mixing and promotes the formation of a stable atmospheric boundary layer, reducing its height. This dampening of the buoyancy driven turbulence effects leads to a stable ABL and stronger vertical temperature gradients. The layer closest to the ground, where surface fluxes are most significant, is referred to as the surface layer. Atmospheric boundary layers

In this situ experiment, the atmospheric boundary layer is analyzed from data gathered from a meteorological station. This meteorology station is used to measure typical atmospheric variables, such as air temperature, pressure, humidity and radiative fluxes. This allows a reconstruction of the diurnal cycle and surface energy balance. In addition, a sonic anemometer is added to measure at a higher frequency wind velocity and temperature. This high frequency and directional wind data is necessary to properly characterize the turbulent flow within the surface layer. The purpose of this report is to analyze these measurements and characterize the structure of the atmospheric boundary layer. Particular emphasis will be placed on thermal stratification, turbulent flow and how they evolve under evolving atmospheric conditions.

6.3 Instrumentation

The meteorological station is situated at approximately 1170 meters altitude and is in a flat field on Grand Colon Mountain. This experiment utilized 3 different types of instrumentation; thermocouples, sonic anemometer and a IR radiation sensor. Air temperature is measured using a resistance-based temperature probe, which relates electrical resistance to temperature. Relative humidity is obtained from a capacitive sensor whose dielectric properties vary with water vapor content. Atmospheric pressure is measured using a piezo resistive sensor sensitive to changes in air pressure. Long wave radiative fluxes are measured using infrared radiometers, allowing estimation of surface radiative cooling. The sonic anemometer uses 6 coupled sonic anemometers to measure the wind velocity in three directions. These coupled anemometers act as both speakers and microphones which they alternate after each signal pass. Wind speed is measured by sending out high frequency sound wave from the speaker to the receiver placed in front of it. Since the distance is known the change in time for the signal to reach the receiver, with taking into account the air temperature, can be converted into a wind speed. The three vectors of wind speed are measured at 20hz.

6.4 Results

The meteorological station was left running for 16 days, with the anemometers running for only 4 days. This difference in time for the data collection was due to to the limited power available on the site, with the weather station being prioritized over the anemometers. Due to this the remainder of this discussion will focus on the 4 days in which both systems were running and powered.

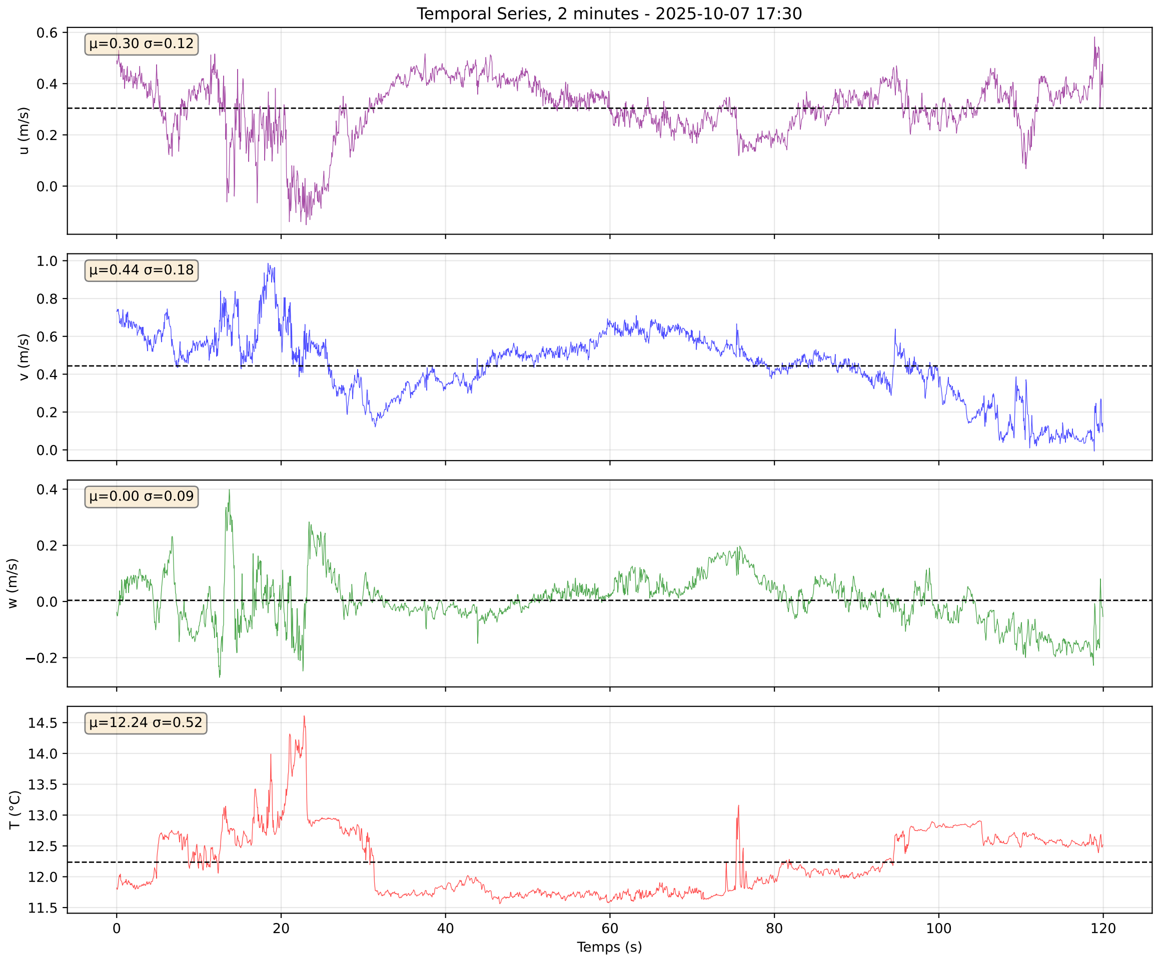

Figure 7: This figure displays a 2 minute snapshot of the sonic emitter's data taken at 20hz. The wind velocity fluctuates drastically enough to validate turbulent flow. This figure also shows a direct correlation with wind velocity fluctuation and air temperature.

Figure 7 shows a two-minute time series of the wind velocity components (u, v, w) and air temperature. The large standard deviation of the velocity signals indicates turbulent flow, and the velocity fluctuations are directly correlated with temperature variations.

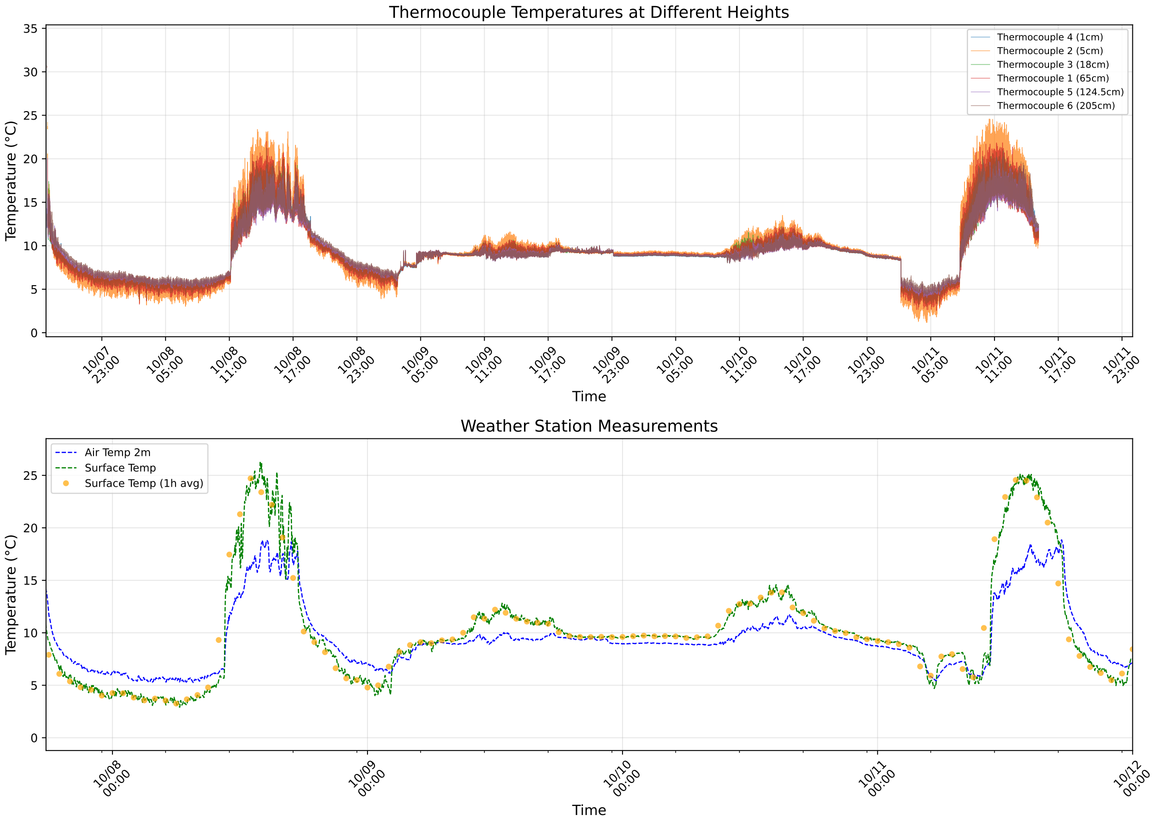

Figure 8: This graph compares the air and surface temperature of the meteorological station with the thermocouple temperatures. Thermocouple data was gathered from 07/10/25 17:45 to 11/10/25 16:30 due to power limitations.

Figure 8 compares the thermocouple measurements with data from the meteorological station; only periods during which the thermocouples were powered are shown. A strong correlation between the two datasets is observed, as expected. In addition, a clear thermal inversion associated with the diurnal cycle is evident. This phenomenon is further analyzed in 9.

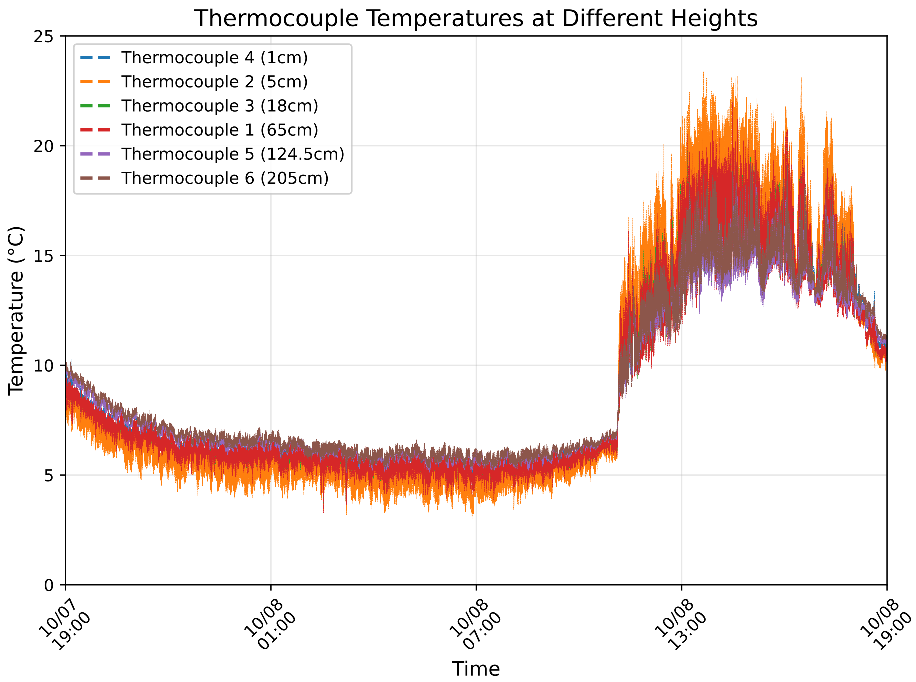

Figure 9: A zoom-in of Figure 8 shows the thermocouple measurements over a 24-hour period. A clear thermal stratification is observed, which reverses during nighttime.

Figure 9 presents a zoomed view of a 24-hour period from the thermocouple measurements shown in Figure 8. The temperature profiles reveal a logarithmic thermal stratification during daytime conditions. During nighttime, this stratification weakens and inverts, indicating a reversal of the vertical temperature gradient over the diurnal cycle.

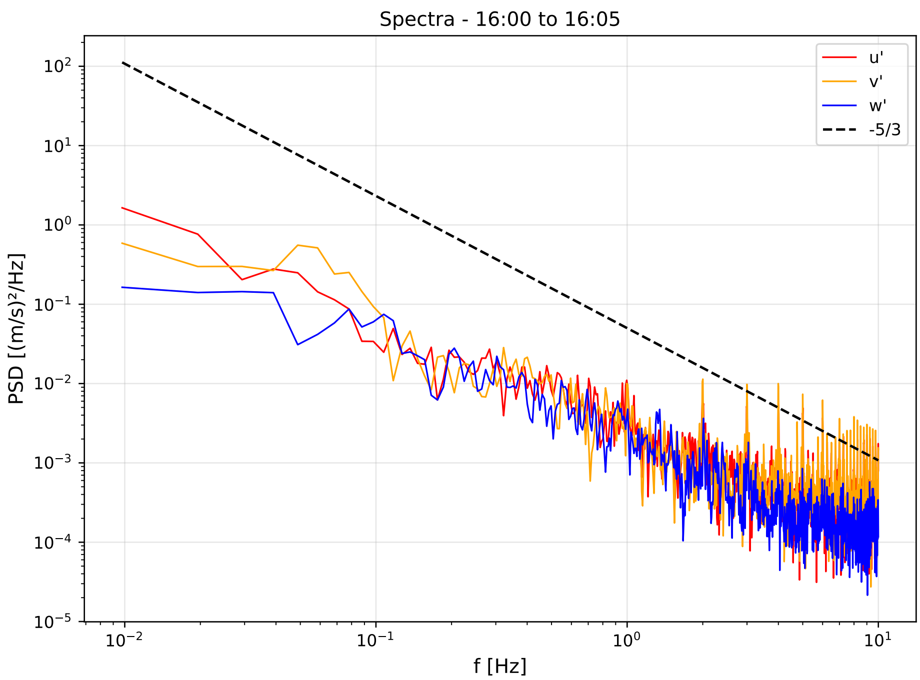

Figure 10: Power Spectral Density of the data acquired from the sonic anemometer. Note the -5/3 slope corresponding to K41.

Figure 10 shows the power spectral density of the sonic anemometer. Given the sampling rate of 20 Hz, the Nyquist frequency is 10 Hz, and only frequencies below this limit are physically meaningful. The PSD exhibits a clear Kolmogorov inertial cascade, further highlighting the importance of accounting for turbulence in atmospheric flow analysis.

Overall, the measurements consistently highlight the coupling between turbulent velocity fluctuations and temperature, as well as the strong influence of the diurnal cycle on the thermal structure of the near-surface atmosphere.

6.5 Conclusion

Studying the atmospheric boundary layer is difficult due to its inherently turbulent nature and its strong dependence on surface conditions. As observed in this in-situ experiment, thermal stratification plays a key role in controlling temperature profiles, turbulent intensity, and vertical mixing within the boundary layer. In-situ measurements of meteorological variables and high-frequency turbulence provided valuable insight into the structure of a near-surface atmospheric boundary layer under stable conditions. The results highlight the importance of accounting for stability effects and surface–atmosphere interactions when analyzing and modeling atmospheric boundary layer flows.

References

[1] N. Machicoane, G. Ricard, R. Osuna-Orozco *et al.*, "Flow structures and dynamics in turbulent multiphase flows," *International Journal of Multiphase Flow*, vol. 129, 103318, 2020.

[2] E. Hopfinger and J.-A. Toly, "Spatially decaying turbulence and its relation to mixing across density interfaces," *Journal of Fluid Mechanics*, vol. 78, pp. 155–175, 1976.

[3] N. Mordant, A. M. Crawford, and E. Bodenschatz, "Three-dimensional structure of the Lagrangian acceleration in turbulent flows," *Physical Review Letters*, vol. 93, 214501, 2004.

[4] C. Charrondière, *Vents catabatiques sur forte pente alpine*, Master M2 Thesis, Université Grenoble Alpes, Grenoble, 2018.

[5] S. Kuksin, "Kolmogorov's theory of turbulence and its rigorous 1D model," *Annales Mathématiques du Québec*, vol. 46, no. 1, pp. 181–193, 2021.

[6] C. Charrondière, C. Brun, J.-M. Cohard *et al.*, "Katabatic winds over steep slopes: Overview of a field experiment designed to investigate slope-normal velocity and near-surface turbulence," *Boundary-Layer Meteorology*, vol. 182, pp. 29–54, 2022.